

Diagnostic Capability of Gadoxetate Disodium-enhanced Liver MRI for Diagnosis of Hepatocellular Carcinoma: Comparison with Multi-detector CT

Naoyuki TOYOTA¹⁾, Yuko NAKAMURA²⁾, Masashi HIEDA¹⁾, Naoko AKIYAMA¹⁾, Hiroaki TERADA¹⁾, Noriaki MATSUURA¹⁾, Masayo NISHIKI¹⁾, Hiroataka KONO³⁾, Hiroshi KOHNO³⁾, Toshimitsu IREI⁴⁾, Yukinobu YOSHIKAWA⁴⁾, Kazuya KURAOKA⁵⁾, Kiyomi TANIYAMA⁵⁾ and Kazuo AWAI²⁾

- 1) Department of Diagnostic Radiology, National Hospital Organization Kure Medical Center and Chugoku Cancer Center, 3-1 Aoyama-cho, Kure 737-0023, Japan
- 2) Department of Diagnostic Radiology, Institute of Biomedical & Health Sciences, Hiroshima University Hospital, 1-2-3 Kasumi, Minami-ku, Hiroshima 734-8551, Japan
- 3) Department of Gastroenterology, National Hospital Organization Kure Medical Center and Chugoku Cancer Center, 3-1 Aoyama-cho, Kure 737-0023, Japan
- 4) Department of Surgery, National Hospital Organization Kure Medical Center and Chugoku Cancer Center, 3-1 Aoyama-cho, Kure 737-0023, Japan
- 5) Department of Pathology, National Hospital Organization Kure Medical Center and Chugoku Cancer Center, 3-1 Aoyama-cho, Kure 737-0023, Japan

ABSTRACT

The purpose of this study was to evaluate the diagnostic capability of gadoxetate disodium (Gd-EOB)-MRI for the detection of hepatocellular carcinoma (HCC) compared with multidetector CT (MDCT). Fifty patients with 57 surgically proven HCCs who underwent Gd-EOB-MRI and MDCT from March 2008 to June 2011 were evaluated. Two observers evaluated MR and CT on a lesion-by-lesion basis. We analyzed sensitivity by grading on a 5-point scale, the degree of arterial enhancement and the differences in histological grades in the diffusion-weighted images (DWI). The results showed that the sensitivity of Gd-EOB-MRI was higher than that of MDCT especially for HCCs that were 1 cm in diameter or smaller. The hepatobiliary phase was useful for the detecting of small HCC. We had few cases in which it was difficult to judge HCC in the arterial enhancement between MRI and MDCT. In the diffusion-weighted image, well differentiated HCC tended to show a low signal intensity, and poorly differentiated HCC tended to show a high signal intensity. In moderately differentiated HCC's, the mean diameter of the high signal intensity group was larger than that of the low signal intensity group (24.5 mm vs. 15.8 mm). In conclusion, Gd-EOB-MRI tended to show higher sensitivity compared to MDCT in the detection of HCC.

Key words: Gadoxetate disodium (EOB), Hepatocellular carcinoma (HCC), Multi-detector row CT (MDCT)

Gadoxetate disodium (EOB-Primovist®, Bayer Yakuhin Ltd., Osaka, Japan; [Gd-EOB]) is a recently introduced hepatocyte-specific contrast agent used for the diagnosis of hepatic tumors by magnetic resonance imaging (MRI). Gd-EOB-enhanced MRI (Gd-EOB-MRI) offers advantages over MRI enhanced with conventional Gd agents because it yields information on hepatocyte function in the hepatobiliary phase (HBP) and on the hepatic blood flow in the vascular phase including the arterial, portal and transitional phase^{2,7,10,12,23}.

Metastatic liver tumors are low-intense in the HBP and the sensitivity for the detection of metastatic liver tumors of Gd-EOB-MRI is superior to multidetector CT^{9,19,22,23}. The sensitivity of Gd-EOB-MRI for the detection of hepatocellular carcinoma

(HCCs) is reported to be higher than of helical computed tomography (CT)^{2,7,9,19,22,23,31}. However, the identification of HCC on Gd-EOB-MRI scans is more complex than of metastatic tumors. During the arterial phase (AP), some HCC nodules are enhanced while others are not; in HBP, some are hypo- and others are hyper-intense^{17,24,28}. Moreover, evaluation of lesion vascularity (i.e. hypervascular or hypovascular) as well as detection of the focal lesion are essential elements of diagnosis of HCC through imaging because a hepatic mass larger than 1 cm in diameter in a cirrhotic liver that demonstrates a typical vascular pattern (arterial hypervascularity and 'wash out' in the equilibrium phase) on CT or MR imaging can be diagnosed as HCC without biopsy^{4,5}. Some concern exists that

Gd-EOB may show weaker enhancement because the volume of Gd-EOB injected is smaller (eg, 6.0 mL/60 kg of body weight for a dose of 25 μ mol/kg) than that of extracellular gadolinium chelated (12.0 mL/60 kg of body weight for a dose of 100 μ mol/kg)¹.

The purpose of this study is to clarify retrospectively the diagnostic capability of Gd-EOB-MRI for the detection and characterization of HCCs compared with multi-detector CT (MDCT).

MATERIALS AND METHODS

Institutional review board approval was obtained for this retrospective study and informed consent was waived.

Study Population

We retrospectively reviewed fifty patients with HCC who underwent hepatic dynamic MRI with Gd-EOB and MDCT from March 2008 to June 2011. There were 32 men and 18 women (age range: 50-89 years; mean age: 68.8 years). All 50 patients had undergone hepatic surgery and their diagnoses of 57 HCCs were based on histopathologic evidence. There was an average interval between MR imaging and MDCT imaging of 24 days (range, 3-74 days); in 38 patients MDCT was performed prior to Gd-EOB-MRI (average interval 23 days).

All patients had a clinical history of chronic liver disease, and the underlying etiology of chronic liver disease was hepatitis C (n = 26), hepatitis B (n = 18), NASH (non-alcoholic steatohepatitis) (n = 2), alcoholic hepatitis (n = 1), and cryptogenic hepatitis or cirrhosis (n = 3). The hepatic function was classified as Child-Pugh A or B in 49 and 1 patient(s), respectively: Hepatic function was also classified as Liver damage A or B in 40 and 10 patients, respectively.

Imaging Technique

MR imaging

All examinations were performed with a 1.5-Tesla MR scanner (Intera Achieva Pulsar, Philips Medical Systems, Best, Netherlands) with a Sense body coil 4ch in 35 cases, and a 1.5-Tesla MR scanner (A-series single gradient, Philips Medical Systems, Best, Netherlands) with a Sense XL torso coil 16ch in 15 cases.

For all patients, before injection of Gd-EOB, T1-weighted two-dimensional dual gradient-recalled echo (GRE) MR imaging (repetition time (TR)/echo time (TE) 218 ms/2-4 msec, flip angle 80°, field of view 35-40 cm, matrix 256 \times 192, slice thickness 6 mm, bandwidth 488.3 Hz/pixel and acquisition time 16.3 sec) was performed.

Dynamic MRI was with fat-suppressed T1-weighted gradient-echo imaging with liver acquisition with volume acceleration [THRIVE]. The parameters for image acquisition were section thickness 2 mm

and interval 0 mm, TR/TE 4.2 msec/shortest 2.0 msec, FA10°, field-of-view (FOV) 37.5 cm, matrix 188 \times 148, parallel imaging factor 2, acquisition time 16.3 sec. All images were obtained in the transverse plane.

After pre-enhanced scanning, Gd-EOB was injected intravenously at a dose of 25 μ mol/kg as a bolus at a rate of 2.0 mL/s and flushed with 20-mL saline using a power injector (Sonic Shot 50; Nemoto Kyorindo, Tokyo, Japan), and 4-phase Gd-EOB-enhanced scans of the liver were acquired during the arterial (AP), portal venous (1 min later), transitional (3 min later), and hepatobiliary phases (HBP) (20 min later). Scanning delays from abdominal aortic contrast arrival to the central k-space acquisition for the arterial phase was 14 sec and we defined the transitional phase as the 180 sec after the start of Gd-EOB injection²³.

All patients underwent single-breath hold, fat-suppressed T2-weighted- and diffusion-weighted imaging (T2-WI, DWI). The parameters for DWI were TR/TE 1200 msec/70 msec, echo train length 192, slice thickness and gap 6/1 mm, matrix size 112 \times 90, parallel imaging factor 2, number of excitations 4, b-value 800 s/mm².

Contrast-enhanced MDCT

All patients were scanned using a 64-detector (Aquillion 64; Toshiba Medical Systems, Tochigi, Japan) or a 128-detector CT instrument (Somatom Definition AS 128, Siemens Healthcare, Erlangen, Germany) at the following settings: rotation time, 0.5 sec for Aquillion 64 and 0.6 sec for SOMATOM; beam collimation, 64 \times 0.5 mm; section thickness and intervals, 5.0 mm; helical pitch (beam pitch), 0.703; table movement, 45 mm/s, scanning FOV, 35 cm; voltage, 120 kV; and auto mA (noise index 8).

Three-phase contrast-enhanced CT images of the liver were obtained during the hepatic arterial phase (HAP) and equilibrium phase (EP). An automatic bolus-tracking program was used to time the start of scanning for each phase after contrast injection. The trigger threshold level was set at 200 Hounsfield units in the abdominal aorta at the L1 vertebral body level. HAP and EP scanning was started at 15 and 145 sec.

The contrast dose for all patients was 600 mgI/kg of their body weight. The contrast material was administered using a power injector (Dual Shot, Nemoto Kyorindo, Tokyo, Japan) and a 20-gauge iv catheter inserted into an antecubital vein. The injection duration was 30 sec in all patients.

Image Analysis

Two board-certified radiologists with 23 and 18 years of experience with abdominal imaging, respectively, evaluated the MRI and CT images. They knew the patients' risk of HCC but knew nothing about other clinical information.

Criteria of HCC on MDCT

HCC was diagnosed if two criteria were met: (a) the lesion was seen to be enhanced clearly during HAP and (b) the lesion was hypo-attenuated with respect to the surrounding liver during the equilibrium phase^{4,7}. Because these criteria are highly specific but not very sensitive⁸, if the lesion was hypo-attenuated with respect to the surrounding liver during the equilibrium phase^{3,6,30}, it was considered to indicate HCC.

Criteria of HCC on Gd-EOB-MRI

At Gd-EOB-MRI during AP some HCC nodules are and others are not enhanced; in HPB some are hypo- and others are hyper-intense^{17,24,28}. HCC was diagnosed if two criteria were met: (a) the lesion was seen to become clearly enhanced during AP and (b) the lesion was hypo-intense during the hepatobiliary phase^{11,17}. Because these criteria are highly specific but not very sensitive, if the lesion was hypo-intense with respect to the surrounding liver during the hepatobiliary phase it was considered to be suggestive of HCC²⁷. The radiologists also evaluated the signal intensity (SI) of the hepatic tumors on DWI because in these sequences, even a mild increase in the SI of hepatic tumors may be suggestive of HCC²³ and a combination of Gd-EOB-MR imaging and DW imaging was reported to yield better diagnostic accuracy and sensitivity in the detection of HCCs than any MR imaging technique alone^{14,16,18,25}.

Comparisons of the degree of enhancement of HCC in the arterial phase between MR and MDCT were also performed. We defined the degree of enhancement using the following 4-point scale: 1, invisible or hypovascular lesions; 2, isointense/dense during the arterial phase and low intense/dense on precontrast MRI/CT, suggesting possible hypervascularity; 3, slightly hyperintense/dense during the arterial phase and necessary to see the precontrast MRI/CT to identify hypervascular lesions; and 4, hypervascularity detected with confidence without seeing the precontrast MRI/CT¹.

Each observer recorded the presence and the location of lesions using a 5-point confidence score for suggestive of HCC: 1, no HCC present; 2, probably no HCC present; 3, equivocal; 4, HCC probably present; 5, definite presence of HCC; with confidence scores of 4 and 5 representing a positive diagnosis of HCC.

Statistical Analysis

We calculated the sensitivity of Gd-EOB-MRI and MDCT based on a tumor-by-tumor analysis of pathologically-confirmed tumors. We also performed subset analysis of sensitivity based on the tumor size using 10-, 20- and 30-mm thresholds. The statistical analysis for differences was performed with the Wilcoxon's signed rank test for the sensitivities. Differences of p value <0.05 were

considered significant.

RESULTS

50 patients harbored one HCC and seven patients had two HCCs. The tumor ranged from 6 to 87 mm in diameter (mean diameter, 22.4 mm). Of 57 HCCs, 7 HCCs were 10 mm or less in diameter, 27 were ranged from 11 to 20 mm in diameter, 13 HCCs were ranged from 21 to 30 mm in diameter, and the remaining 10 HCCs were over 31 mm in diameter. Fifty-seven HCCs were further classified as poorly differentiated (n = 12), moderately differentiated (n = 37), or well differentiated (n = 8). The tumor grades of HCC were determined on the basis of the predominating component in the HCC.

Sensitivity for each imaging technique is shown in Table 1. Gd-EOB-MRI showed higher sensitivity in detecting lesions compared to MDCT, with significant difference between the two imaging techniques (p = 0.043 for observer 1 and 0.005 for observer 2).

In the detection of HCC that were 1 cm in diameter or smaller (n = 7), the sensitivity of MRI was much higher than that of MDCT and there was significant difference only for observer 2 (p = 0.068 for observer 1 and 0.043 for observer 2) (Table 1) (Fig. 1). For the detection of HCC larger than 1 cm, the sensitivity of MRI was similar to that of MDCT and there was significant difference only for observer 2 (p = 0.32 for observer 1 and 0.043 for observer 2). Of 7 HCCs smaller than 1 cm, 3 well differentiated HCCs were only detected with Gd-EOB-MRI as hypo-intense during HBP without arterial enhancement.

In the detection of HCC according to histological grades (Table 2), the sensitivity of MRI was higher than MDCT in well- and moderately differentiated HCC; but there was only significant difference for moderately differentiated HCC by observer 2 (p value of well, moderately and poorly differentiated HCCs for observer 1 was 0.32, 0.18, and 1.0, respectively, and for observer 2, 0.11, 0.043, and 0.32, respectively). On DWI by each histological grade (Table 3), most of the well differentiated HCCs were non-visible (62.5%). On the other hand,

Table 1. Sensitivity of EOB-MRI and MDCT in the detection of HCC

Tumor diameter (cm)		MRI	MDCT
≤1	7	85.7 (6)	28.6 (2)
>1-2	27	96.3 (26)	92.6 (25)
>2-3	13	92.3 (12)	92.3 (12)
>3	10	100 (10)	100 (10)
total	57	96.5 (55)	91.2 (52)

Numbers are percentages. Numbers in parentheses are the number of HCCs.

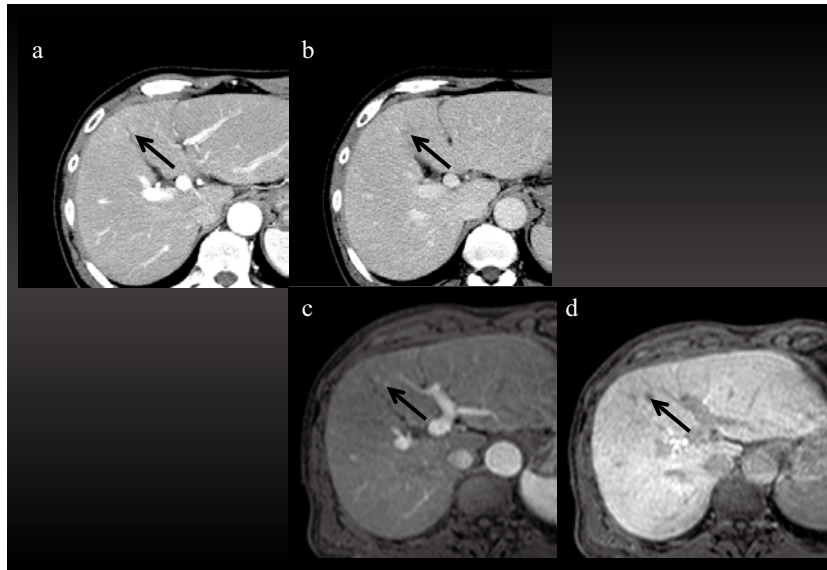


Fig. 1. A 66-year-old man with a 10-mm-diameter well differentiated HCC in segment 4.

(a: AP at MDCT, b: EP at MDCT, c: AP at Gd-EOB-MRI, d: HBP at Gd-EOB-MRI).

Abbreviations: AP, arterial phase; EP, equilibrium phase; HBP, hepatobiliary phase

A: The tumor (arrow) showed arterial enhancement.

B: The tumor showed ambiguous washout pattern of HCC (arrow). This tumor was classified as category 3 at MDCT.

C: The tumor (arrow) showed arterial enhancement at Gd-EOB-MRI.

D: The tumor showed hypointense (arrow) at HBP. The tumor was classified as category 5 at Gd-EOB-MRI.

Table 2. Sensitivity of EOB-MRI and MDCT in the detection of HCC

Histology	Total	MRI	MDCT
well diff.	8	100 (8)	87.5 (7)
moderate diff.	37	97.3 (36)	91.9 (34)
poorly diff.	12	91.7 (11)	91.7 (11)

Numbers are percentages. Numbers in parentheses are the number of HCCs.

Table 3. HCC Detection Rate in Diffusion-Weighted Image by each Histology

Histology	grade 3	grade 2 or 3
well diff.	12.5 % (1/ 8)	37.5 % (3/ 8)
moderately diff.	51.4 % (19/37)	64.9 % (24/37)
poorly diff.	75.0 % (9/12)	91.7 % (11/12)

Numbers are percentages. Numbers in parentheses are the number of HCCs.

grade 1: nonvisible

grade 2: visible by referring with the other sequences

grade 3: high-intensity (easy to detect)

most of the poorly differentiated HCC group showed high-signal intensity (91.7%) on DWI. In moderately differentiated HCCs, the mean diameter of the high signal intensity group was larger than that of the low signal intensity group (24.5 mm vs. 15.8 mm).

We compared the arterial enhancement between Gd-EOB-MRI and MDCT for 50 HCCs. The degree of arterial enhancement of MDCT was more prom-

inent than that of MRI in 13 HCCs (26.5%), the degree of MDCT is equal to that of MRI in 29 HCCs (59.2%), and the degree of enhancement of MRI was more prominent than that of MDCT in 7 HCCs (14.3%).

Concerning sensitivity of HCC according the liver damage classification, there was no significant difference either at Gd-EOB-MRI or at MDCT.

DISCUSSION

Our study revealed that Gd-EOB-MRI showed higher sensitivity for HCC compared to MDCT, with a significant difference. Di Martino et al⁷⁾ reported that Gd-EOB-MRI yields significantly higher diagnostic accuracy and sensitivity in the detection of HCC in patients with cirrhosis compared with 64-MDCT. Our results are compatible with those previous reports.

For lesions 1 cm or smaller, the sensitivity of Gd-EOB-MRI was higher than that of MDCT and there was a significant difference only for observer 2. This was possibly because the number of HCCs smaller than 1 cm was small. Moreover, 3 well differentiated HCCs smaller than 1 cm were only detected with Gd-EOB-MRI as hypo-intense during HBP without arterial enhancement. There are several reports of the superiority of Gd-EOB-MRI compared to MDCT for the detection of small HCCs^{9,12,27)}.

Hammerstingl et al⁹⁾ reported that the highest rate of correctly detected lesions including HCC and metastases with a diameter below 1 cm was

achieved by Gd-EOB-MRI (61.8%) compared with double-phase CT (37.3%). Kim et al¹⁵⁾ reported that 3-Tesla MRI may also be better than triple-phase MDCT for the detection of HCC 1 cm in diameter or smaller. Therefore, Gd-EOB-MRI should be used especially for the detection of small HCC.

In the detection of HCC according to their histological grades, the sensitivity of MRI was higher than MDCT in well- and moderately differentiated HCC. In fact, well differentiated HCCs were only detected with Gd-EOB-MRI as hypo-intense during HBP without arterial enhancement. Kim et al¹⁵⁾ also reported that Gd-EOB-MRI, including the hepatobiliary phase, is more sensitive than MDCT for the detection of HCCs. Sano et al²⁷⁾ also reported that Gd-EOB-MRI, compared to MDCT, is the most useful imaging technique for evaluating small HCCs, specifically owing to its high sensitivity to early HCC. Therefore, Gd-EOB-MRI is considered to be especially useful for the detection of low grade HCCs.

The mean diameter of moderately differentiated HCCs not detected on DWI was smaller compared to that of moderately differentiated HCCs detected on DWI (15.8 mm vs. 24.5 mm). Xu et al²⁹⁾ suggested that the combined use of DWI with dynamic MRI provided higher sensitivities than conventional dynamic MRI alone in the detection of small HCC (≤ 2 cm), although they did not mention the histological grade of HCC. Therefore, when the lesion shows high signal intensity, it could be a poorly or larger moderately differentiated HCC.

Concerning arterial enhancement with Gd-EOB, only four hypervascular 50 HCCs at MDCT (8%) revealed no arterial enhancement at Gd-EOB-MRI. This might be because the amount of gadolinium within Gd-EOB was less than that in other gadolinium cases, because other sequences including hepatobiliary phase and DWI showed typical findings of HCC. Moreover, the degree of arterial enhancement of Gd-EOB-MRI was more prominent than that of MDCT in 7 HCCs (14.3%). Kim et al¹⁵⁾ reported that there were 2 lesions that were seen as hypervascular HCC on Gd-EOB-MRI but not depicted even on triple-phase MDCT. Therefore, the diagnosis of HCC is almost comparable in arterial enhancement between MRI and MDCT.

As Gd-EOB has hepatocyte-selective characteristics, focal hepatic lesions manifest strong contrast during HBP. On the other hand, HBP images are affected by liver dysfunction and enhancement of the liver parenchyma is decreased or heterogeneous in the presence of reduced hepatic function^{20,26)}. In patients with severe liver dysfunction, the contrast between the tumor and the liver parenchyma during HBP was worse and the sensitivity of HCCs may also decrease. Therefore, we determined the difference of sensitivity at Gd-EOB-MRI according to liver damage classification. Our data showed that

there was no statistically significant differences in the sensitivity of HCC among the liver damage classifications. We thought that the hepatobiliary phase was not affected due to mild liver damage, because we had no class C patients.

A small number of HCC show hyperintense in HBP. This is caused by overexpression of OATP 1B3, the sodium-independent organic anion transporter of hepatocytes^{17,24,28)}. Although we had only two hyperintense HCCs (one well- and one moderately differentiated HCC), it was not proved that they overexpressed OATP1B3. We have to keep in mind hyperintense HCC in HBP in reading Gd-EOB-MRI.

Our study had several limitations. First, our study population was relatively small. For an accurate evaluation of tumor extension on both MR images and surgical specimens we selected tumors that were histopathologically confirmed as HCCs. In this sense our findings must be considered preliminary. Second, we used only resected liver specimens as the standard of reference. To determine the diagnostic sensitivity of Gd-EOB-MRI histopathologic study of the whole liver is necessary and pathologic- and MRI findings must be correlated tumor-by-tumor in livers extracted at transplantation or obtained at autopsy. Third, the most important risk factor for HCC is chronic liver disease and liver dysfunction may be severe in some HCC patients, for example, Child-Pugh class C and we had no patients with Child-Pugh C. However, patients with Child-Pugh class C have less opportunity to undergo therapy for HCC especially hepatic resection; therefore, our study population may be applicable in the clinical setting.

In conclusion, overall diagnostic performance of Gd-EOB-MRI is similar to that of MDCT in the preoperative detection of HCC. Moreover, Gd-EOB-MRI yields higher sensitivity than MDCT in the detection of HCCs smaller than 1 cm in diameter and low grade HCCs. Gd-EOB-MRI plays a central role in detecting HCC in preoperative imaging technique.

(Received April 18, 2013)

(Accepted June 4, 2013)

REFERENCES

1. Akai, H., Kiryu, S., Takao, H., Tajima, T., Shibahara, J., Imamura, H., et al. 2009. Efficacy of double-arterial phase gadolinium ethoxybenzyl diethylenetriamine pentaacetic acid-enhanced liver magnetic resonance imaging compared with double-arterial phase multi-detector row helical computed tomography. *J. Comput. Assist. Tomogr.* **33**: 887-892.
2. Bluemke, D.A., Sahani, D., Amendola, M., Balzer, T., Breuer, J., Brown, J.J., et al. 2005. Efficacy and safety of MR imaging with liver-specific contrast agent: U.S. multicenter phase III study. *Radiology* **237**: 89-98.

3. **Bolondi, L., Gaiani, S., Celli, N., Golfieri, R., Francesco, G., Leoni, S., et al.** 2005. Characterization of small nodules in cirrhosis by assessment of vascularity: the problem of hypovascular hepatocellular carcinoma. *Hepatology* **42**: 27-34.
4. **Bruix, J. and Sherman, M.** 2005. Management of hepatocellular carcinoma. *Hepatology* **42**: 1208-1236.
5. **Bruix, J. and Sherman, M.** 2011. Management of hepatocellular carcinoma: an update. *Hepatology* **53**: 1020-1022.
6. **Chung, J.J., Yu, J.S., Kim, J.H., Kim, M.J. and Kim, K.W.** 2008. Nonhypervascular hypoattenuating nodules depicted on either portal or equilibrium phase multiphasic CT images in the cirrhotic liver. *AJR. Am. J. Roentgenol.* **191**: 207-214.
7. **Di Martino, M., Marin, D., Guerrisi, A., Baski, M., Galati, F., Rossi, M., et al.** 2010. Intraindividual comparison of gadoxetate disodium-enhanced MR imaging and 64-section multidetector CT in the detection of hepatocellular carcinoma in patients with cirrhosis. *Radiology* **256**: 806-816.
8. **Forner, A., Vilana, R., Ayuso, C., Bianchi, L., Sole, M., Ayuso, J.R., et al.** 2008. Diagnosis of hepatic nodules 20 mm or smaller in cirrhosis: prospective validation of the noninvasive diagnostic criteria for hepatocellular carcinoma. *Hepatology* **47**: 97-104.
9. **Hammerstingl, R., Huppertz, A., Breuer, J., Balzer, T., Blakeborough, A., Carter, R., et al.** 2008. Diagnostic efficacy of gadoxetic acid (Primovist)-enhanced MRI and spiral CT for a therapeutic strategy: comparison with intraoperative and histopathologic findings in focal liver lesions. *Eur. Radiol.* **18**: 457-467.
10. **Huppertz, A., Balzer, T., Blakeborough, A., Breuer, J., Giovagnoni, A., Heinz-Peer, G., et al.** 2004. Improved detection of focal liver lesions at MR imaging: multicenter comparison of gadoxetic acid-enhanced MR images with intraoperative findings. *Radiology* **230**: 266-275.
11. **Huppertz, A., Haraida, S., Kraus, A., Zech, C.J., Scheidler, J., Breuer, J., et al.** 2005. Enhancement of focal liver lesions at gadoxetic acid-enhanced MR imaging: correlation with histopathologic findings and spiral CT-initial observations. *Radiology* **234**: 468-478.
12. **Ichikawa, T., Saito, K., Yoshioka, N., Tanimoto, A., Gokan, T., Takehara, Y., et al.** 2010. Detection and characterization of focal liver lesions: a Japanese phase III, multicenter comparison between gadoxetic acid disodium-enhanced magnetic resonance imaging and contrast-enhanced computed tomography predominantly in patients with hepatocellular carcinoma and chronic liver disease. *Invest. Radiol.* **45**: 133-141.
13. **Kim, S.H., Kim, S.H., Lee, J., Kim, M.J., Jeon, Y.H., Park, Y., et al.** 2009. Gadoxetic acid-enhanced MRI versus triple-phase MDCT for the preoperative detection of hepatocellular carcinoma. *AJR. Am. J. Roentgenol.* **192**: 1675-1681.
14. **Kim, Y.K., Kim, C.S., Han, Y.M. and Lee, Y.H.** 2011. Detection of liver malignancy with gadoxetic acid-enhanced MRI: is addition of diffusion-weighted MRI beneficial?. *Clin. Radiol.* **66**: 489-496.
15. **Kim, Y.K., Kwak, H.S., Kim, C.S. and Han, Y.M.** 2009. Detection and characterization of focal hepatic tumors: a comparison of T2-weighted MR images before and after the administration of gadoxetic acid. *J. Magn. Reson. Imaging.* **30**: 437-443.
16. **Kim, Y.K., Lee, W.J., Park, M.J., Kim, S.H., Rhim, H. and Choi, D.** 2012. Hypovascular hypointense nodules on hepatobiliary phase gadoxetic acid-enhanced MRI images in patients with cirrhosis: potential of DW imaging in predicting progression to hypervascular HCC. *Radiology* **265**: 104-114.
17. **Kitao, A., Zen, Y., Matsui, O., Gabata, T., Kobayashi, S., Koda, W., et al.** 2010. Hepatocellular carcinoma: signal intensity at gadoxetic acid-enhanced MR imaging-correlation with molecular transporters and histopathologic features. *Radiology* **256**: 817-826.
18. **Lee, M.H., Kim, S.H., Park, M.J., Park, C.K. and Rhim, H.** 2011. Gadoxetic acid-enhanced hepatobiliary phase MRI and high-b-value diffusion-weighted imaging to distinguish well-differentiated hepatocellular carcinomas from benign nodules in patients with chronic liver disease. *AJR. Am. J. Roentgenol.* **197**: W868-875.
19. **Motosugi, U., Ichikawa, T., Morisaka, H., Sou, H., Muhi, A., Kimura, K., et al.** 2011. Detection of pancreatic carcinoma and liver metastases with gadoxetic acid-enhanced MR imaging: comparison with contrast-enhanced multi-detector row CT. *Radiology* **260**: 446-453.
20. **Motosugi, U., Ichikawa, T., Sou, H., Sano, K., Tominaga, L., Kitamura, T., et al.** 2009. Liver parenchymal enhancement of hepatocyte-phase images in Gd-EOB-DTPA-enhanced MR imaging: which biological markers of the liver function affect the enhancement? *J. Magn. Reson. Imaging* **30**: 1042-1046.
21. **Muhi, A., Ichikawa, T., Motosugi, U., Sano, K., Matsuda, M., Kitamura, T., et al.** 2009. High-b-value diffusion-weighted MR imaging of hepatocellular lesions: estimation of grade of malignancy of hepatocellular carcinoma. *J. Magn. Reson. Imaging* **30**: 1005-1011.
22. **Muhi, A., Ichikawa, T., Motosugi, U., Sou, H., Nakajima, H., Sano, K., et al.** 2011. Diagnosis of colorectal hepatic metastases: comparison of contrast-enhanced CT, contrast-enhanced US, superparamagnetic iron oxide-enhanced MRI, and gadoxetic acid-enhanced MRI. *J. Magn. Reson. Imaging* **34**: 326-335.
23. **Nakamura, Y., Toyota, N., Date, S., Oda, S., Namimoto, T., Yamashita, Y., et al.** 2011. Clinical significance of the transitional phase at gadoxetate disodium-enhanced hepatic MRI for diagnosis of hepatocellular carcinoma: preliminary results. *J. Comput. Assist. Tomogr.* **35**: 723-727.
24. **Narita, M., Hatano, E., Arizono, S., Miyagawa-Hayashino, A., Isoda, H., Kitamura, K., et al.** 2009. Expression of OATP1B3 determines uptake of Gd-EOB-DTPA in hepatocellular carcinoma. *J. Gastroenterol.* **44**: 793-798.
25. **Park, M.J., Kim, Y.K., Lee, M.W., Lee, W.J., Kim, Y.S., Kim, S.H., et al.** 2012. Small hepatocellular carcinomas: improved sensitivity by combining gadoxetic acid-enhanced and diffusion-weighted MR imaging patterns. *Radiology* **264**: 761-770.
26. **Reimer, P., Rummeny, E.J., Shamsi, K., Balzer, T.,**

- Daldrup, H.E., Tombach, B., et al.** 1996. Phase II clinical evaluation of Gd-EOB-DTPA: dose, safety aspects, and pulse sequence. *Radiology* **199**: 177-183.
27. **Sano, K., Ichikawa, T., Motosugi, U., Sou, H., Muhi, A.M., Matsuda, M., et al.** 2011. Imaging study of early hepatocellular carcinoma: usefulness of gadoteric acid-enhanced MR imaging. *Radiology* **261**: 834-844.
28. **Tsuboyama, T., Onishi, H., Kim, T., Akita, H., Hori, M., Tatsumi, M., et al.** 2010. Hepatocellular carcinoma: hepatocyte-selective enhancement at gadoteric acid-enhanced MR imaging-correlation with expression of sinusoidal and canalicular transporters and bile accumulation. *Radiology* **255**: 824-833.
29. **Xu, P.J., Yan, F.H., Wang, J.H., Lin, J. and Ji, Y.** 2009. Added value of breathhold diffusion-weighted MRI in detection of small hepatocellular carcinoma lesions compared with dynamic contrast enhanced MRI alone using receiver operating characteristic curve analysis. *J. Magn. Reson. Imaging* **29**: 341-349.
30. **Yu, J.S., Chung, J.J., Kim, J.H. and Kim, K.W.** 2008. Large (≥ 2 cm) non-hypervascular nodules depicted on MRI in the cirrhotic liver: fate and implications. *Clin. Radiol.* **63**: 1121-1130.
31. **Zech, C.J., Hermann, K.A., Reiser, M.F. and Schoenberg, S.O.** 2007. MR imaging in patients with suspected liver metastases: value of liver-specific contrast agent Gd-EOB-DTPA. *Magn. Reson. Med. Sci.* **6**: 43-52.